



Spin splitting in low-symmetry quantum wells beyond Rashba and Dresselhaus terms

G. V. Budkin  and S. A. Tarasenko
Ioffe Institute, 194021 St. Petersburg, Russia (Received 7 February 2022; revised 21 March 2022; accepted 24 March 2022; published 7 April 2022)

Spin-orbit interaction in semiconductor structures with broken space inversion symmetry leads to spin splitting of electron and hole states even in the absence of magnetic field. We discover that, beyond the Rashba and Dresselhaus contributions, there is an additional type of the zero-field spin splitting which is caused by the interplay of the cubic shape of crystal unit cell and macroscopic structure asymmetry. In quantum wells grown along low-symmetry crystallographic axes, this type of spin-orbit interaction couples the out-of-plane component of carrier's spin with the in-plane momentum whereas the coupling strength is controlled by structure inversion asymmetry. We carry out numerical calculations and develop an analytical theory, which demonstrate that this interaction dominates k -linear spin splitting of heavy-hole subbands in a wide range of parameters.

DOI: [10.1103/PhysRevB.105.L161301](https://doi.org/10.1103/PhysRevB.105.L161301)

Zero-field spin splitting of electron and hole subbands in semiconductors caused by spin-orbit (SO) interaction gives rise to a variety of exciting phenomena which are being explored for technological applications [1–3]. Examples are the intrinsic and intrinsic inverse spin Hall effects [4,5], the spin-galvanic effect [6–9], and spin orientation by electric current [10,11], persistent spin helices [12–14], and the paradigmatic spin field-effect transistor [15,16].

Two contributions to the zero-field spin splitting in zinc-blende-type quantum wells (QWs) are commonly considered: the Rashba and Dresselhaus terms [17–19]. The Rashba (or Bychkov-Rashba) SO interaction [20–25] is related to the QW structure inversion asymmetry (SIA) which can be tuned by an electric field applied along the QW normal. The effective magnetic field \mathbf{B}_R corresponding to the Rashba splitting lies in the QW plane. The Dresselhaus term originates from bulk inversion asymmetry (BIA) of the underlying crystal [26–30]. The corresponding effective magnetic field \mathbf{B}_D is tied to the crystallographic axes and, therefore, its direction depends on the QW crystallographic orientation [27]. In particular, \mathbf{B}_D lies in the QW plane in (001)-oriented structures whereas it points along the QW normal in (110)-oriented structures.

Technological achievements and the search for new physics stimulate the study of QWs grown along low-symmetry axes, such as [012], [013], etc. [31–33]. Whereas the analysis of atomic structure readily shows that the symmetry of such QWs is reduced (down to the trivial C_1 group compared to the C_{2v} group of (001)-grown QWs [34]) and, therefore, additional terms in the SO Hamiltonian get phenomenologically allowed, it is commonly assumed that the SO Hamiltonian still consists of the Rashba and Dresselhaus terms. The latter is obtained from the bulk Dresselhaus term by the proper projection onto two-dimensional states in the coordinate frame relevant to the QW.

Here, we show that there is an additional term in the Hamiltonian of zero-field splitting, which emerges in any QW except those grown along the high-symmetry axes (001),

(011), and (111). The term is relevant for QWs based on cubic crystals, e.g., both zinc-blende-type and diamond-type crystals, and does not require bulk inversion asymmetry. The effective magnetic field corresponding to this type of SO splitting points along the QW normal whereas its magnitude is controlled by structure inversion asymmetry and can be tuned by gate voltage. Moreover, we find that this SO interaction dominates the k -linear spin splitting of heavy-hole (HH) subbands in low-symmetry QWs based on III–V semiconductors, such as (013)-grown GaAs QWs. In the framework of the Luttinger Hamiltonian, we construct the effective Hamiltonian of the HH SO splitting for (01*h*)-grown QWs where l and h are the Miller indices and study how the SO splitting depends on the QW orientation and width as well as the electric field applied along the growth direction. Calculations also reveal that the k -linear Rashba splitting of the HH states, which is absent in the isotropic approximation and emerges in the cubic model, has a strong dependence on the QW crystallographic orientation.

First, we show that k -linear SO splitting follows from symmetry consideration and construct the effective Hamiltonian. Figure 1 sketches the microscopic structures of asymmetric QWs grown from a cubic crystal along three different [01*h*] axes: [001], [012], and [011]. The crystal unit cells are shown by cubes, the color gradient from blue to red illustrates the QW structure inversion asymmetry. We focus on the cubicity of the unit cell and neglect its internal structure, in particular, bulk inversion asymmetry for zinc-blende-type crystals. Moreover, for heavy holes in asymmetric quantum wells, the BIA term is typically smaller than the SIA term [25].

Figure 1 reveals that the symmetry of a QW depends on its crystallographic orientation if the cubicity of unit cells is taken into account. The highest symmetry, corresponding to the C_{4v} point group in the cubic model, is achieved for (001)-grown QWs, Fig. 1(a). Such a symmetry allows for k -linear Rashba splitting of conduction-band electrons (particles with the spin projections $\pm 1/2$ on the QW normal) and

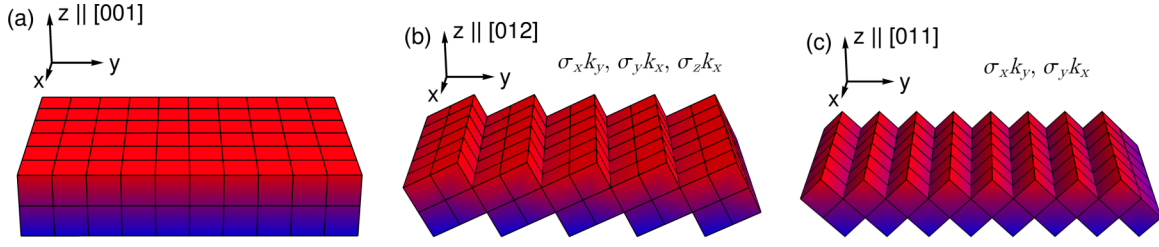


FIG. 1. Sketch of the microscopic structures of QWs grown from a cubic crystal along the [001], [012], and [011] axes. The cubic symmetry of crystal unit cells together with structure inversion asymmetry gives rise to \mathbf{k} -linear spin splitting of the HH subband in (012)- and (011)-grown QWs with the terms shown in the figure.

\mathbf{k} -cubic Rashba splitting of heavy holes (particles with the spin projections $\pm 3/2$). \mathbf{k} -linear Rashba splitting of HH is absent in this model and is known to be tiny in real (001)-grown zinc-blende-type QWs [17]. In (011)-grown QWs [Fig. 1(c)], the in-plane axes x and y get nonequivalent and the effective symmetry is reduced to the C_{2v} point group. This symmetry enables \mathbf{k} -linear coupling of the $\pm 3/2$ states. As the results, the Rashba Hamiltonian for HH acquires \mathbf{k} -linear terms and becomes anisotropic.

QWs grown along any axes between [001] and [011], e.g., (012)-grown QWs as shown in Fig. 1(b), has lower symmetry. In the cubic model, they are described by the C_s point group with the only nontrivial symmetry element: the mirror plane $x \rightarrow -x$. In addition to the anisotropic Rashba term, the SO Hamiltonian in such QWs may contain the unusual term $\sigma_z k_x$ which is also invariant in the C_s point group. Thus, the effective Hamiltonian of \mathbf{k} -linear SO interaction in (012)-grown QWs of the C_s symmetry can be generally presented in the form

$$H_{\text{SO}} = \alpha_1 \sigma_y k_x - \alpha_2 \sigma_x k_y + \zeta \sigma_z k_x, \quad (1)$$

where α_1 , α_2 , and ζ are the SO coupling parameters, $\sigma_{x,y,z}$ are the Pauli matrices, $k_{x,y}$ are the in-plane wave-vector components, and $x \parallel [100]$, $y \parallel [0h\bar{l}]$, and $z \parallel [0lh]$ are the coordinate axes relevant to (012)-grown QWs. Below, we calculate these parameters for the HH subband and demonstrate that for most crystallographic orientations the term $\sigma_z k_x$ dominates. This term seems to be responsible for the out-of-plane spin polarization of surface states in (013)-grown HgTe/CdHgTe topological insulators observed in our numerical $\mathbf{k} \cdot \mathbf{p}$ calculations [35]. Note that a similar term caused by BIA in (012)-grown QWs would have the form $\sigma_z k_y$ [36].

Now, we develop a microscopic theory of SO splitting. The Γ_8 valence band in bulk cubic semiconductors is described by the Luttinger Hamiltonian, which in the cubic axes has the form [17,34]

$$H_L = \frac{\hbar^2}{2m_0} \left[- \left(\gamma_1 + \frac{5}{2} \gamma_2 \right) \mathbf{k}^2 + 2\gamma_2 (\mathbf{J}\mathbf{k})^2 + 2(\gamma_3 - \gamma_2) \sum_{i \neq j} (J_i k_i) (J_j k_j) \right], \quad (2)$$

where γ_1 , γ_2 , and γ_3 are the Luttinger parameters, \mathbf{k} is the three-dimensional wave vector, and \mathbf{J} is the vector composed of the matrices of the angular momentum $3/2$.

To calculate the dispersion of valence subbands in (012)-grown QW, we rotate the Luttinger Hamiltonian in the QW coordinate frame (x, y, z) and solve the Schrödinger equation $H\Psi = E\Psi$ with the Hamiltonian,

$$H = H_L^{(i)} + H_L^{(a)} + eV(z), \quad (3)$$

where $H_L^{(i)}$ and $H_L^{(a)}$ are the isotropic and anisotropic parts of the Luttinger Hamiltonian, respectively, and $eV(z)$ is the electrostatic potential energy [35]. We use the simplest form of boundary conditions at the QW interfaces: the continuity of Ψ and $v_z \Psi$ at the interfaces, where $v_z = \hbar^{-1} \partial H_L / \partial k_z$. These boundary conditions applied to (012)-grown structures correspond to the Hamiltonians,

$$H_L^{(i)} = \frac{\hbar^2}{2m_0} \left[-\mathbf{k} \left(\gamma_1 + \frac{5}{2} \gamma_2 \right) \mathbf{k} + 2 \sum_{ij} \{J_i J_j\}_s k_i \gamma_2 k_j \right], \quad (4)$$

and

$$H_L^{(a)} = \frac{2\hbar^2}{m_0} \left\{ \{J_x J_y\}_s (\gamma_3 - \gamma_2) k_x k_y + \{J_x J_z\}_s \{ \gamma_3 - \gamma_2, k_z \}_s k_x + \left[\{J_y J_z\}_s \cos 2\theta + \frac{J_z^2 - J_y^2}{2} \sin 2\theta \right] \times \left[\{ \gamma_3 - \gamma_2, k_z \}_s k_y \cos 2\theta + \frac{k_z (\gamma_3 - \gamma_2) k_z - (\gamma_3 - \gamma_2) k_y^2}{2} \sin 2\theta \right] \right\}, \quad (5)$$

where $\mathbf{k}_{\parallel} = (k_x, k_y)$ is the in-plane wave vector, $k_z = -i\partial_z$, $\{AB\}_s = (AB + BA)/2$ is the symmetrized product, $\theta = \arctan(l/h)$ is the angle between the QW growth direction [012] and the [001] axis, and the Luttinger parameters may now depend on the z coordinate.

The energy spectra of the ground HH subband in (001)-, (012)-, and (011)-grown GaAs/AlAs QWs are shown in Fig. 2. The spectra are calculated using the Luttinger parameters listed in Table I and the valence-band offset between GaAs and AlAs 590 meV [38]. The electrostatic potential

TABLE I. Luttinger parameters of GaAs and AlAs [37].

	γ_1	γ_2	γ_3
GaAs	6.98	2.06	2.93
AlAs	3.76	0.82	1.42

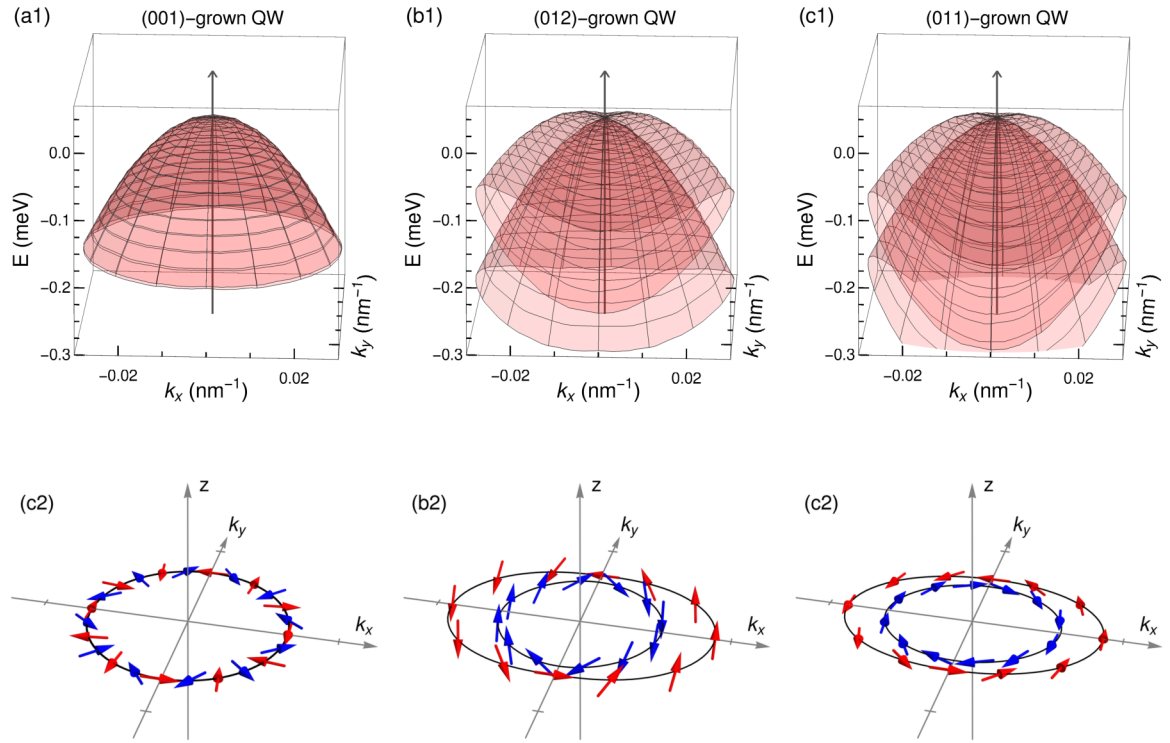


FIG. 2. (a1), (b1), and (c1) Energy spectra of ground heavy-hole subband in (001)-, (012)-, and (011)-grown GaAs/AlAs QWs, respectively. (a2), (b2), and (c2) Equipotential cross sections of the energy spectra. Red and blue arrows show the orientations of heavy-hole pseudospin in the spin subbands. Calculations are carried out for 5-nm-wide QWs with the built-in electric field $E_z = 400$ kV/cm.

$V(z)$ is set to constants in the barriers and $V(z) = E_z z$ inside the well.

Figures 2(a1), 2(b1), and 2(c1) reveal that the HH spin-orbit splitting dramatically depends on the QW crystallographic orientation. As expected, the splitting is negligible in (001)-grown QWs where k -linear terms are absent and the Rashba splitting emerges only in the third order in the wave vector [17]. In contrast, anisotropic k -linear splitting of the HH subband is clearly observed in the energy spectra of (012)- and (011)-grown QWs. Moreover, among all the QW orientations considered in Fig. 2, the splitting is maximal in the (012)-grown QW. This is most clearly seen in Figs. 2(a2), 2(b2), and 2(c2), where solid black lines show the equipotential cross sections of the energy spectra.

To clarify the nature of the observed SO splitting we calculate the directions of pseudospin in the spin subbands. The pseudospin in state Ψ is defined as $s = \chi^\dagger \sigma \chi$, where $\chi = (a, b)^T / \sqrt{|a|^2 + |b|^2}$ with a and b being the expansion coefficients of Ψ in the HH ground states $|\pm 3/2\rangle$. Blue and red arrows in Figs. 2(a2), 2(b2), and 2(c2) show the pseudospin orientations as a function of the in-plane wave-vector k_{\parallel} for (001)-, (012)-, and (011)-grown QWs, respectively. In the (011)-grown QW [Fig. 2(c2)], the pseudospin lies in the QW plane. In line with the symmetry consideration, the overall dependence of spin splitting on k_{\parallel} is described by the anisotropic Rashba Hamiltonian given by the first two terms in Eq. (1). The striking difference of SO interaction in the (012)-grown QW [Fig. 2(c2)], compared to (001)- and (011)-grown structures, is that the pseudospin s has both the in-plane and out-of-plane components. Physically, it means that the eigenstates are formed mostly from either $|+3/2\rangle$

or $|-3/2\rangle$ states. In accordance with the symmetry analysis, such a kind of SO splitting is allowed in cubic QWs grown along low-symmetry axes, see Fig. 1. Moreover, the numerical calculations show that, in the (012)-grown QW, s points mostly along the QW normal for $k \parallel x$ where the spin splitting is maximal. All the observed features are well described by the effective Hamiltonian (1) with $|\zeta| > |\alpha_1|, |\alpha_2|$.

We perform a series of numerical calculations to obtain the dependence of the SO coupling parameters α_1 , α_2 , and ζ on the the QW width and crystallographic orientation. The results are summarized in Fig. 3. The dependences of the SO parameters on the QW width turn out to be nonmonotonic and have maxima at around 7 nm. In narrower QWs, the influence of the electric field E_z , which is set to the constant in the QW and zero in the barriers, on the HH states is reduced. As a result, the SO parameters decrease. In wide QWs, the SO parameters tend to the constants since the well effectively becomes triangular with the slope eE_z .

The inset in Fig. 3(a) shows the dependence of the SO parameters on angle θ which defines the QW crystallographic orientation. The angles $\theta = 0$ and $\theta = \pi/4$ correspond to (001)-grown and (011)-grown QWs, respectively. In line with the symmetry consideration, the parameters are zero at $\theta = 0$ and $\zeta = 0$ at $\theta = \pi/4$. The parameters α_1 , α_2 are proportional to θ^2 at small θ and reach maxima at $\theta = \pi/4$, i.e., in (110)-grown QWs. The parameter ζ behaves differently: It is proportional to θ at small angles and reaches a maximum at $\theta \approx 0.36$ which is close to the (013)-growth direction. The calculations show that for GaAs/AlAs QWs the term $\zeta \sigma_z k_x$ prevails in the SO Hamiltonian of heavy holes in a wide range of QW crystallographic orientations.

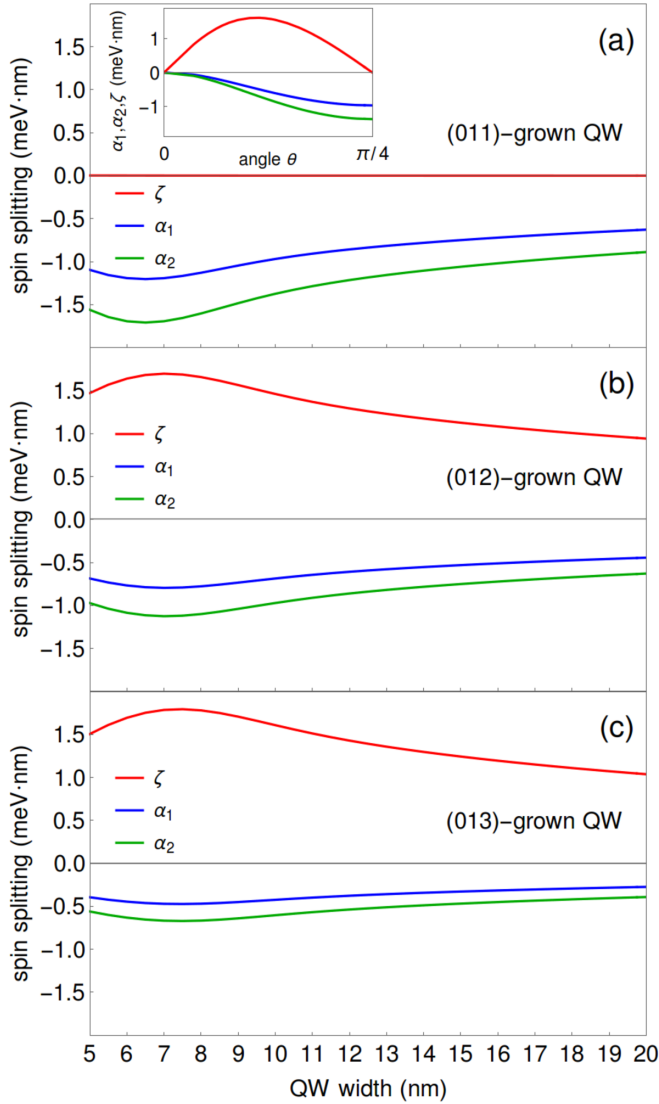


FIG. 3. Dependences of the parameters of SO Hamiltonian (1) α_1 , α_2 , and ζ of heavy holes on the QW width for (011)-, (012)-, and (013)-grown GaAs/AlAs QWs. The dependences are calculated for the Luttinger parameters listed in Table I and built-in electric field $E_z = 100$ kV/cm. The inset shows the dependence of α_1 , α_2 , and ζ on the growth direction θ for 10-nm-wide QWs.

Finally, we obtain analytical expressions for the SO coupling parameters. We assume that the warping of the valence-band spectrum, which is an essential ingredient for the \mathbf{k} -linear splitting of the HH subbands, is small, i.e., $|\gamma_2 - \gamma_3| \ll \bar{\gamma}$, where $\bar{\gamma} = (\gamma_2 + \gamma_3)/2$.

At $\mathbf{k}_{\parallel} = 0$ and in the absence of warping ($H_L^{(a)} = 0$), the solution of the Schrödinger equation gives the series of the heavy-hole and light-hole states $|HHn, \pm 3/2\rangle$ and

$|LHn, \pm 1/2\rangle$, respectively, with the energies $\varepsilon_{h/l,n}$ and the envelop functions $\varphi_{h/l,n}(z)$.

At $\mathbf{k}_{\parallel} \neq 0$, the ground HH states $|HH1, +3/2\rangle$ and $|HH1, -3/2\rangle$ are coupled. The \mathbf{k} -linear coupling is described by the effective Hamiltonian (1). The second-order perturbation theory (first order in \mathbf{k}_{\parallel} and first order in $\gamma_2 - \gamma_3$) gives the following equations for the SO coupling parameters (see Ref. [39] for details),

$$\alpha_{1,2} = \frac{3\hbar^2 Q}{2m_0} \sin^2 2\theta, \quad \zeta = -\frac{3\hbar^2 Q}{2m_0} \sin 4\theta, \quad (6)$$

where

$$Q = \frac{\hbar^2}{m_0} \sum_n \frac{\int \varphi_{h,1}(z) \{\bar{\gamma}, \partial_z\}_s \varphi_{l,n}(z) dz}{\varepsilon_{h,1} - \varepsilon_{l,n}} \times \int \varphi_{l,n}(z) \partial_z (\gamma_3 - \gamma_2) \partial_z \varphi_{h,1}(z) dz. \quad (7)$$

The parameter Q is nonzero only if the QW is asymmetric and, at least, one of the Luttinger parameters has a jump at the interfaces [40].

The dependences of α_1 , α_2 , and ζ on the growth direction θ calculated numerically in Fig. 3 are well described by Eqs. (6) despite the fact that the analytical theory is not strictly applicable to GaAs/AlAs QWs since the difference between γ_2 and γ_3 is not small. As it follows from Eqs. (6), the parameter ζ reaches a maximum at $\theta = \pi/8$ which is quite close to 0.36 obtained in the numerical calculations.

To summarize, we have shown that the zero-field spin splitting of two-dimensional states in QWs grown along low-symmetry crystallographic axes goes beyond the Rashba and Dresselhaus contributions. In particular, there is spin-orbit coupling between the out-of-plane component of the carrier's spin and the in-plane momentum whose strength is governed by QW structure inversion asymmetry. The developed microscopic theory shows that this type of coupling can be quite strong and dominate \mathbf{k} -linear spin splitting of heavy holes in $(0lh)$ -oriented GaAs QWs. This finding provides an additional way to manipulate spins in low-dimensional structures.

More generally, our Letter suggests a type of tunable gyrotropy in low-symmetry QW structures: coupling between the out-of-plane component of an axial vector and the in-plane component of a polar vector controlled by structure inversion asymmetry. This coupling can give rise to a number of interesting phenomena, such as optical activity, magnetoelectric effect, current-induced Faraday and Kerr rotation, the circular photogalvanic effect, etc.

G.V.B. acknowledges support from the Russian Science Foundation (Project No. 21-72-10035) and the "BASIS" Foundation.

- [1] D. D. Awschalom and M. E. Flatté, Challenges for semiconductor spintronics, *Nat. Phys.* **3**, 153 (2007).
 [2] J. Fabian, A. Matos-Abiague, C. Ertler, P. Stano, and I. Žutić, Semiconductor spintronics, *Acta Physica Slovaca* **57**, 565 (2007).

- [3] *Spin Physics in Semiconductors*, edited by M. I. Dyakonov (Springer-Verlag, Berlin, 2008).
 [4] J. Sinova, S. O. Valenzuela, J. Wunderlich, C. H. Back, and T. Jungwirth, Spin Hall effects, *Rev. Mod. Phys.* **87**, 1213 (2015).

- [5] M. Kimata, H. Chen, K. Kondou, S. Sugimoto, P. K. Muduli, M. Ikhlas, Y. Omori, T. Tomita, A. H. MacDonald, S. Nakatsuji, and Y. Otani, Magnetic and magnetic inverse spin Hall effects in a non-collinear antiferromagnet, *Nature (London)* **565**, 627 (2019).
- [6] E. L. Ivchenko, Y. B. Lyanda-Geller, and G. E. Pikus, Current of thermalized spin-oriented photocarriers, *JETP* **71**, 550 (1990).
- [7] S. D. Ganichev, E. L. Ivchenko, V. V. Bel'kov, S. A. Tarasenko, M. Sollinger, D. Weiss, W. Wegscheider, and W. Prettl, Spin-galvanic effect, *Nature (London)* **417**, 153 (2002).
- [8] S. A. Tarasenko, A. V. Poshakinskiy, E. L. Ivchenko, I. Stepanov, M. Ersfeld, M. Lepsa, and B. Beschoten, Zitterbewegung of spin split electrons, *JETP Lett.* **108**, 326 (2018).
- [9] D. Khokhriakov, A. M. Hoque, B. Karpik, and S. P. Dash, Gate-tunable spin-galvanic effect in graphene-topological insulator van der Waals heterostructures at room temperature, *Nat. Commun.* **11**, 3657 (2020).
- [10] B. M. Norman, C. J. Trowbridge, D. D. Awschalom, and V. Sih, Current-Induced Spin Polarization in Anisotropic Spin-Orbit Fields, *Phys. Rev. Lett.* **112**, 056601 (2014).
- [11] S. D. Ganichev, M. Trushin, and J. Schliemann, *Handbook of Spin Transport and Magnetism*, Spin Orientation by Electric Current (Chapman and Hall, Boca Raton, FL, 2020).
- [12] J. Schliemann, Colloquium: Persistent spin textures in semiconductor nanostructures, *Rev. Mod. Phys.* **89**, 011001 (2017).
- [13] M. Kohda and G. Salis, Physics and application of persistent spin helix state in semiconductor heterostructures, *Semicond. Sci. Technol.* **32**, 073002 (2017).
- [14] F. Passmann, S. Anghel, C. Ruppert, A. D. Bristow, A. V. Poshakinskiy, S. A. Tarasenko, and M. Betz, Dynamical formation and active control of persistent spin helices in III-V and II-VI quantum wells, *Semicond. Sci. Technol.* **34**, 093002 (2019).
- [15] S. Datta and B. Das, Electronic analog of the electro-optic modulator, *Appl. Phys. Lett.* **56**, 665 (1990).
- [16] P. Chuang, S.-C. Ho, L. W. Smith, F. Sfigakis, M. Pepper, C.-H. Chen, J.-C. Fan, J. P. Griffiths, I. Farrer, H. E. Beere, G. A. C. Jones, D. A. Ritchie, and T.-M. Chen, All-electric all-semiconductor spin field-effect transistors, *Nat. Nanotechnol.* **10**, 35 (2015).
- [17] R. Winkler, *Spin-Orbit Coupling Effects in Two-Dimensional Electron and Hole Systems* (Springer, Berlin, 2003).
- [18] W. Zawadzki and P. Pfeffer, Spin splitting of subband energies due to inversion asymmetry in semiconductor heterostructures, *Semicond. Sci. Technol.* **19**, R1 (2004).
- [19] Additional contributions to SO splitting may come from interface inversion asymmetry [41–44] and strain [28]. The former is typically small and plays a role if other sources of SO interaction are suppressed, such as in symmetric Si/Ge QWs [45], or if electron/hole states are bound to interfaces, such as in HgTe/CdHgTe topological insulators [46]. Strain, particularly shear strain in lattice-mismatched (110)-grown QWs, can significantly increase the SO splitting and make the Rashba splitting anisotropic [36,47].
- [20] E. I. Rashba, Properties of semiconductors with an extremum loop. I. Cyclotron and combinational resonance in a magnetic field perpendicular to the plane of the loop, *Sov. Phys. Solid State* **2**, 1109 (1960).
- [21] F. T. Vasko, Spin splitting in the spectrum of two-dimensional electrons due to the surface potential, *JETP Lett.* **30**, 541 (1979).
- [22] Y. A. Bychkov and E. Rashba, Properties of a 2D electron gas with lifted spectral degeneracy, *JETP Lett.* **39**, 78 (1984).
- [23] R. Winkler, Rashba spin splitting in two-dimensional electron and hole systems, *Phys. Rev. B* **62**, 4245 (2000).
- [24] A. Manchon, H. C. Koo, J. Nitta, S. M. Frolov, and R. A. Duine, New perspectives for Rashba spin-orbit coupling, *Nat. Mater.* **14**, 871 (2015).
- [25] E. Marcellina, A. R. Hamilton, R. Winkler, and D. Culcer, Spin-orbit interactions in inversion-asymmetric two-dimensional hole systems: A variational analysis, *Phys. Rev. B* **95**, 075305 (2017).
- [26] G. Dresselhaus, Spin-orbit coupling effects in zinc blende structures, *Phys. Rev.* **100**, 580 (1955).
- [27] M. I. D'yakonov and V. Y. Kachorovskii, Spin relaxation of conduction electrons in noncentrosymmetric semiconductors, *Sov. Phys. Semicond.* **20**, 110 (1986).
- [28] G. E. Pikus, V. A. Maruschak, and A. N. Titkov, pin splitting of energy bands and spin relaxation of carriers in cubic iii-v crystals, *Sov. Phys. Semicond.* **22**, 115 (1988).
- [29] E. Rashba and E. Sherman, Spin-orbital band splitting in symmetric quantum wells, *Phys. Lett. A* **129**, 175 (1988).
- [30] M. V. Durnev, M. M. Glazov, and E. L. Ivchenko, Spin-orbit splitting of valence subbands in semiconductor nanostructures, *Phys. Rev. B* **89**, 075430 (2014).
- [31] S. Dvoretzky, N. Mikhailov, D. Ikusov, V. Kartashev, A. Kolesnikov, I. Sabinina, Y. G. Sidorov, and V. Shvets, The growth of CdTe layer on GaAs substrate by MBE, in *Methods for Film Synthesis and Coating Procedures* (IntechOpen, London 2020).
- [32] K. Nakanishi, A. Arikawa, Y. Saito, D. Iizasa, S. Iba, Y. Ohno, N. Yokota, M. Kohda, Y. Ishitani, and K. Morita, Room-temperature spin-orbit magnetic fields in slightly misoriented (110) InGaAs/InAlAs multiple quantum wells, *Appl. Phys. Lett.* **119**, 032405 (2021).
- [33] X. Lu, N. Kumagai, Y. Minami, and T. Kitada, Sublattice reversal in GaAs/Ge/GaAs heterostructures grown on (113)b GaAs substrates, *Appl. Phys. Express* **11**, 015501 (2017).
- [34] E. Ivchenko, *Optical Spectroscopy of Semiconductor Nanostructures* (Alpha Science, Exton, PA, 2005).
- [35] K.-M. Dantscher, D. A. Kozlov, P. Olbrich, C. Zoth, P. Faltermeier, M. Lindner, G. V. Budkin, S. A. Tarasenko, V. V. Bel'kov, Z. D. Kvon, N. N. Mikhailov, S. A. Dvoretzky, D. Weiss, B. Jenichen, and S. D. Ganichev, Cyclotron-resonance-assisted photocurrents in surface states of a three-dimensional topological insulator based on a strained high-mobility HgTe film, *Phys. Rev. B* **92**, 165314 (2015).
- [36] M. O. Nestoklon, S. A. Tarasenko, R. Benchamekh, and P. Voisin, Spin splitting of electron states in lattice-mismatched (110)-oriented quantum wells, *Phys. Rev. B* **94**, 115310 (2016).
- [37] M. Sodagar, M. Khoshnagar, A. Eftekharian, and S. Khorasani, Exciton-photon interaction in a quantum dot embedded in a photonic microcavity, *J. Phys. B: At. Mol. Opt. Phys.* **42**, 085402 (2009).
- [38] Y. Wang, F. Zahid, Y. Zhu, L. Liu, J. Wang, and H. Guo, Band offset of GaAs/Al_xGa_{1-x}As heterojunctions from atomistic first principles, *Appl. Phys. Lett.* **102**, 132109 (2013).
- [39] See Supplemental Material at <http://link.aps.org/supplemental/10.1103/PhysRevB.105.L161301> for details of the perturbation theory.

- [40] See Supplemental Material at <http://link.aps.org/supplemental/10.1103/PhysRevB.105.L161301> for the proof that the SO coupling parameters vanish if the Luttinger parameters have no spatial dependence.
- [41] E. L. Ivchenko, A. Y. Kaminski, and U. Rössler, Heavy-light hole mixing at zinc-blende (001) interfaces under normal incidence, *Phys. Rev. B* **54**, 5852 (1996).
- [42] O. Krebs, D. Rondi, J. L. Gentner, L. Goldstein, and P. Voisin, Inversion Asymmetry in Heterostructures of Zinc-Blende Semiconductors: Interface and External Potential Versus Bulk Effects, *Phys. Rev. Lett.* **80**, 5770 (1998).
- [43] R. Magri and A. Zunger, Anticrossing and coupling of light-hole and heavy-hole states in (001) GaAs/Al_xGa_{1-x}As heterostructures, *Phys. Rev. B* **62**, 10364 (2000).
- [44] Zh. A. Devizorova, A. V. Shchepetilnikov, Yu. A. Nefyodov, V. A. Volkov, and I. V. Kukushkin, Interface contributions to the spin-orbit interaction parameters of electrons at the (001) GaAs/AlGaAs interface, *JETP Lett.* **100**, 102 (2014).
- [45] M. O. Nestoklon, L. E. Golub, and E. L. Ivchenko, Spin and valley-orbit splittings in SiGe/Si heterostructures, *Phys. Rev. B* **73**, 235334 (2006).
- [46] S. A. Tarasenko, M. V. Durnev, M. O. Nestoklon, E. L. Ivchenko, J.-W. Luo, and A. Zunger, Split Dirac cones in HgTe/CdTe quantum wells due to symmetry-enforced level anticrossing at interfaces, *Phys. Rev. B* **91**, 081302(R) (2015).
- [47] J.-X. Xiong, S. Guan, J.-W. Luo, and S.-S. Li, Emergence of strong tunable linear Rashba spin-orbit coupling in two-dimensional hole gases in semiconductor quantum wells, *Phys. Rev. B* **103**, 085309 (2021).